

Diffraction-limited 76 mas speckle masking observations of the core of NGC 1068 with the SAO 6 m telescope ^{*}

M. Wittkowski^{1,2}, Y. Balega³, T. Beckert², W.J. Duschl^{2,1}, K.-H. Hofmann¹, and G. Weigelt¹

¹ Max-Planck-Institut für Radioastronomie, Auf dem Hügel 69, D-53121 Bonn, Germany

² Institut für Theoretische Astrophysik, Tiergartenstraße 15, D-69121 Heidelberg, Germany

³ Special Astrophysical Observatory, Nizhnij Arkhyz, Zelenchuk region, Karachai-Cherkesia, 357147, Russia

Received ...; accepted ...

Abstract. We present the first K-band bispectrum speckle interferometry of NGC 1068 with an angular resolution of 76 mas (~ 5.5 pc). This angular resolution allows us to attribute the measured flux to only one of the nuclear sources seen at radio wavelengths. The observed decreasing visibility function suggests that the dominant central core is probably not an unresolved point source, but slightly resolved with a FWHM diameter of ~ 30 mas ~ 2 pc for an assumed Gaussian intensity distribution. This 30 mas object is possibly the nuclear torus and/or a scattering halo.

We discuss different contributions to the observed K band flux. Between 5 GHz and the K-band the spectrum of this component is close to a $\nu^{1/3}$ proportionality. In addition to the standard interpretation of a hot dust torus surrounding the nucleus of NGC 1068, one cannot exclude the possibility that a sizeable fraction of the nuclear flux reaches us via a scattering halo. This then would allow us to determine physical parameters of the nuclear source.

Key words: techniques: interferometric – galaxies: fundamental parameters – galaxies: nuclei – galaxies: photometry – galaxies: Seyfert – galaxies: individual: NGC 1068

1. Introduction

The Seyfert 2 galaxy NGC 1068 is one of the nearest and brightest Seyfert galaxies and thus one of the closest candidates for an actively accreting supermassive black hole. Its distance is about 15 Mpc, corresponding to 73 pc $''$. Cores of Seyfert galaxies are classified as types 1 and 2, with type 1 exhibiting broad and narrow lines while the spectra of type 2 show only narrow lines. Unified theories of AGN propose that all AGN harbour a continuum source surrounded by a dusty molecular torus. Depending on the observer's viewing angle this torus either obscures the view on the inner source (type 2), or it does

not (type 1) (Antonucci and Miller 1985). For NGC 1068 Bailey et al. (1988) find from NIR spectroscopy a rather low A_V , perhaps as small as $A_V \sim 10^m$. The extinction is wavelength-dependent and much less in the near infrared, allowing for a deeper look towards type 2 cores in the IR. Accordingly, the first high-resolution IR observations of NGC 1068 exhibited a spectacular compact central IR core and an underlying galaxy (Chelli et al. 1987; Blietz et al. 1994; Tacconi et al. 1994; Young et al. 1996; Weinberger, Neugebauer, Matthews 1996; Quirrenbach, Eckart, Thatte 1997; Thatte et al. 1997).

Recent investigations of the center of *our* Galaxy indicate that the difference between it and a Seyfert core is not of a generic nature but rather a question of the *current* level of activity (Mezger, Duschl, Zylka 1996 = MDZ96). For our Galactic Center it was shown by Duschl and Lesch (1994) and – in more detail – by Beckert et al. (1996 = BDM96) that the radio-IR spectrum of the central source Sgr A* can be explained as optically thin synchrotron radiation of quasi-monoenergetic relativistic electrons. The spectrum is characterized by a flux density $F_\nu \propto \nu^{1/3}$ between a maximum flux in the FIR range and a low frequency turnover at ~ 1 GHz due to synchrotron self-absorption (SSA).

Recently, Muxlow et al. (1996 = MPH96) have presented spectacular MERLIN interferometry observations of the central radio structure of NGC 1068 between 5 and 22 GHz. They have separated the core into 5 components with a minimum distance between individual components of ~ 100 mas. All but one of the components show negative spectral indices $dF_\nu/d\nu$ between -0.33 and -0.88 , while the remaining component shows a positive index of $+0.31$. MPH96 identify this component as the true center of NGC 1068, in so far as resembling the nuclear source of our Galaxy, Sgr A*.

In this letter we present speckle masking bispectrum observations of the core of NGC 1068 in the K-band with a resolution of 76 mas, give the flux at 2.2 μ m, and discuss the nuclear radio-IR spectrum of this Seyfert galaxy.

2. Observations and data reduction

The NGC 1068 speckle interferograms were obtained with the 6 m telescope at the Special Astrophysical Observatory (SAO)

Send offprint requests to: Markus Wittkowski, Bonn; E-Mail: mw@speckle.mpifr-bonn.mpg.de

^{*} Based on data collected at the Special Astrophysical Observatory, Russia

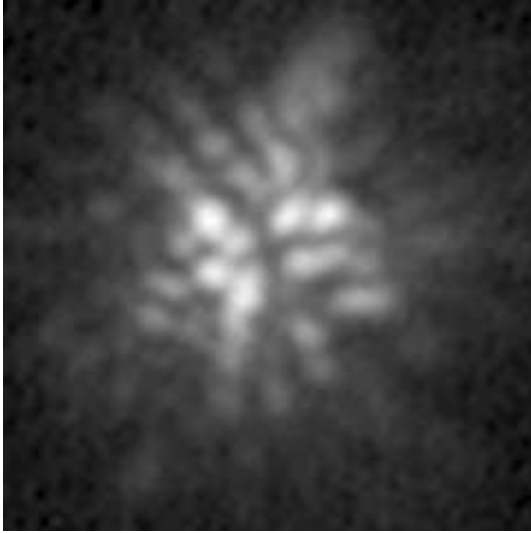


Fig. 1. One of our 778 speckle interferograms of NGC 1068 taken through a K-band filter, demonstrating that it is possible to obtain speckles with high signal-to-noise ratio from a $K \sim 8$ source, even under not very good seeing conditions. The observations were made using a NICMOS 3 array with 200 ms exposure time per frame and multiple read-out ($4\times$). Furthermore, the high-contrast speckles show that the NGC 1068 core is very compact since the speckles look like speckles of a point source. The shown field of view is $1''.85 \times 1''.85$.

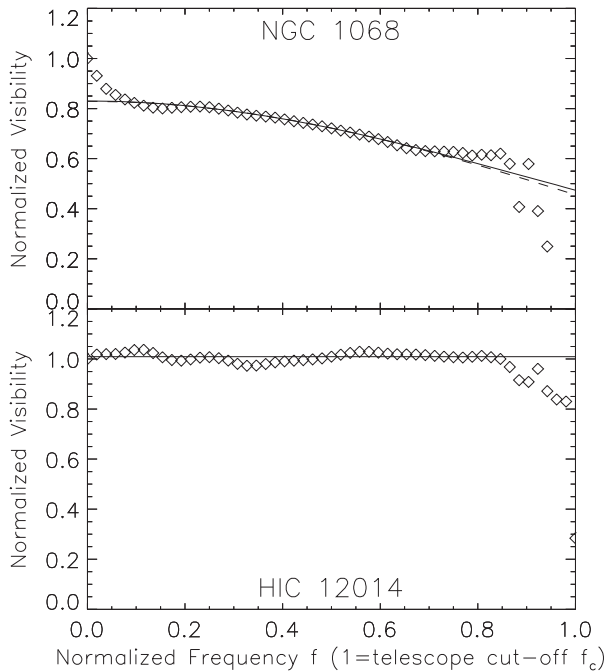


Fig. 2. Azimuthally averaged visibilities of NGC 1068 (top) and the unresolved reference star HIC 12014 (bottom). The diamonds indicate the observed visibilities, the solid lines the Gaussian fits, while the dashed line is a UD fit. The fit range is between 20 % and 70 % of the telescope cut-off frequency f_c . The visibility errors at 20 %, 50 %, 70 %, 80 % and 90 % of f_c are ± 0.05 , ± 0.05 , ± 0.08 , ± 0.15 , ± 0.20 , respectively.

in Russia on October 3, 1996. The speckle interferograms were recorded with a 256×256 pixel NICMOS 3 camera through a standard K-band filter with center wavelength of 2191 nm and FWHM bandwidth of 411 nm. A typical speckle frame is shown in Fig. 1. The exposure time per frame was 200 ms, K-band seeing was about $1''.5$. 778 object speckle interferograms and 526 reference star (HIC 12014) interferograms were recorded. The scale was 30.82 mas/pixel and the field of view $7''.9 \times 7''.9$. Diffraction-limited images were reconstructed from the speckle data using the speckle masking method (Weigelt 1977; Lohmann, Weigelt, Wirtzner 1983; Pehlemann, Hofmann, Weigelt 1992). The process includes the calculation of the average power spectrum and the average bispectrum and the subtraction of the detector noise terms from those. The 4-dimensional bispectrum of each frame consisted of ~ 49 million elements. No postprocessing by image restoration methods was applied to the speckle masking reconstructions. For the calibration of the flux the photometric standard star HIC 110609 (= BS 8541), chosen from Elias et al. (1982), was observed on September 30, 1996. We adopt the HIC 110609 flux to be 12.57 Jy at $2.2 \mu\text{m}$.

3. Results

The top diagram of Fig. 2 shows the azimuthally averaged visibility function of NGC 1068 together with the corresponding uniform-disk (UD) and Gaussian fits. The object visibility function was obtained by compensating both, the seeing-calibrated speckle transfer function and an additional transfer function due to the different spectra of NGC 1068 and the reference star HIC 12014 (K0). On the bottom diagram the analogous plots are shown for the reference star HIC 12014. The HIC 12014 visibility function was obtained by reducing two different data sets of HIC 12014. The reconstructed visibility function of NGC 1068 decreases to about 50 % of the zero-frequency value at the diffraction cut-off frequency f_c . The low-frequency peak is caused by the underlying galaxy. It is not yet clear whether the short horizontal part of the visibility function at $f > 0.7 f_c$ is caused by an additional point source or by an overestimation of the transfer function due to the different spectra of NGC 1068 and the reference star. The decrease of the NGC 1068 visibility function is much larger than the errors (see caption of Fig. 2). For example, between 10 % and 70 % of f_c the visibility function decreases by about 25 %, which is approximately three times larger than the 8 % error at 70 % of f_c . Nevertheless, future observations will be useful to confirm the result and to improve the accuracy.

The diameter of the resolved NGC 1068 core was derived from the reconstructed visibility function by fitting symmetric uniform disks (UD) and Gaussian models. The fits were carried out in the range between 20 % and 70 % of f_c . The fitted diameters d_{Gauss} (FWHM) and d_{UD} of the Gaussian and the UD model are $d_{\text{Gauss}} = 30 \text{ mas} \pm 8 \text{ mas}$ and $d_{\text{UD}} = 50 \text{ mas} \pm 15 \text{ mas}$. These diameters correspond to $2.2 \text{ pc} \pm 0.5 \text{ pc}$ and $3.7 \text{ pc} \pm 0.8 \text{ pc}$, respectively. An alternative model interpretation of the decreasing visibility function is, for exam-

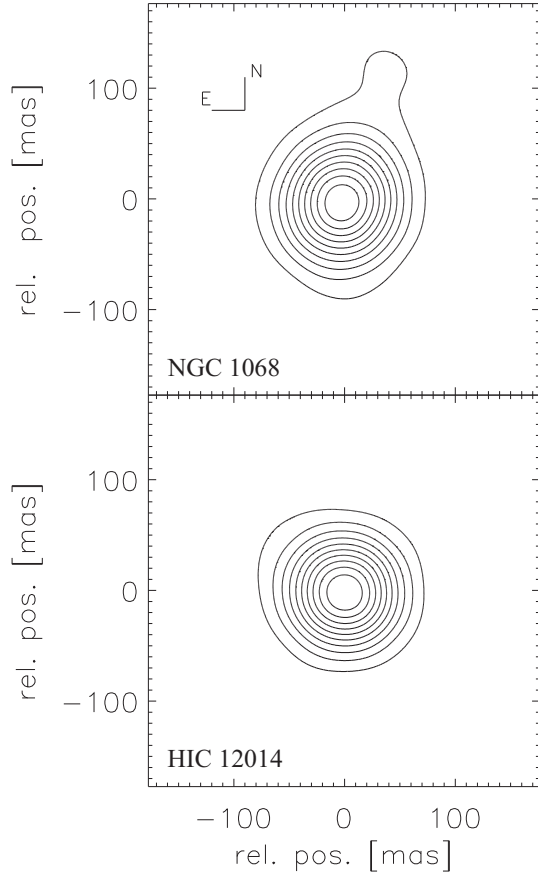


Fig. 3. Diffraction-limited speckle masking reconstruction of NGC 1068 (top) and the unresolved star HIC 12014 (bottom). The contours are plotted from 6% to 100% of peak intensity in 10 steps.

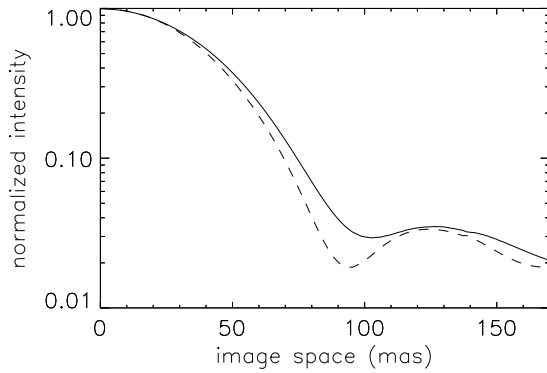


Fig. 4. Azimuthally averaged radial plots of the reconstructed images of NGC 1068 (solid line) and the reference star HIC 12014 (dashed line).

ple, an object slightly larger than the above diameters plus an unresolved central object or an object which is unresolved in one direction (\sim EW), but resolved in the direction perpendicular to it (\sim NS).

Figure 3 shows the diffraction-limited speckle masking reconstruction of NGC 1068. The resolution of the reconstructed image is 76 mas. It shows an elongated structure in the north-northeast direction, i.e. approximately the position of the radio jet. Figure 4 shows the azimuthally averaged radial plots of the reconstructions.

Photometry was performed by comparing the integral intensities of the long-exposure images of NGC 1068 and the photometric standard star HIC 110609. It yields for the flux F_ν of NGC 1068 in the K-band the value $F_K = 650 \text{ mJy} \pm 200 \text{ mJy}$. From this value we have to subtract the flux of the underlying faint extended component in order to get the flux $F_K^{30 \text{ mas}}$ of only the 30 mas component. We determine the contribution of this extended component from the zero-frequency visibility peak discussed above to $20\% \pm 10\%$ of F_K . This results in a flux from the 30 mas component of $F_K^{30 \text{ mas}} = 520 \text{ mJy} \pm 210 \text{ mJy}$.

4. The radio-IR spectrum of the inner parsecs of NGC 1068

MPH96 showed that the central $\sim 2''$ have substructures on a scale of 100 mas requiring observations with a resolution of better than 100 mas to separate the true nuclear spectrum from that of surrounding sources. Only a few published radio flux determinations of the nucleus of NGC 1068 have a sufficiently high angular resolution to allow the separation of individual nuclear components and thus to use it for physical investigations of the nucleus' property. Fortunately, our speckle observations have the required high angular resolution (76 mas). Therefore, our resolution would allow the separation of the individual core components discussed by MPH96 if present in the IR. We assume that the single source that we have observed in the K-band is the same as the true nucleus observed by MPH96. Our observations constitute an upper limit to the volume from which the above determined $520 \text{ mJy} \pm 210 \text{ mJy}$ originate.

Usually, the K band flux from nuclei of Seyfert 2 galaxies is attributed either to a warm dust torus or a compact nuclear stellar cluster or a combination of the two (e.g., Thatte et al. 1997). If our source is the torus that is held responsible for the different appearances of Seyfert 1 and 2 galaxies, our observation constitute the first determination of a torus size. To clarify the nature of the radiating source, further spectroscopic and polarimetric measurements with a similarly high angular resolution are necessary.

However, a combination of the flux measurements and nuclear source identification by MPH96 in the radio frequency regime with our observation makes it intriguing to speculate whether a sizable fraction of $F_K^{30 \text{ mas}}$ could originate from the very nucleus of NGC 1068 rather than from the torus. This could be achieved in a scattering halo above and below the nuclear torus. In this halo a large part of the flux could be isotropically scattered rather than absorbed and thermalized in an opaque torus along our direct line-of-sight to the nucleus. $F_K^{30 \text{ mas}}$ lies only about a factor of two above the extrapolated $F_\nu \propto \nu^{1/3}$ spectrum derived for the range around 10 GHz: The

spectral index $dF_\nu/d\nu$ between 5 GHz and the K band amounts to ≤ 0.39 . We note that this value is very similar to that of other galactic nuclei, like Sgr A* (BDM96), M 81 (Reuter and Lesch 1996); M 104 (Jauch and Duschl, in prep.), where $\alpha = 1/3$. If NGC 1068 has the same spectral shape as these other galactic nuclei, then a fraction of $F_K^{30\text{mas}}$ could indeed be contributed from the nucleus of NGC 1068.

However, one has to admit that very little is known about the true nuclear spectrum of NGC 1068 in the intermediate frequency range. To pursue our speculation, we assume – as a working hypothesis – that also between 22 GHz and the IR range, the spectrum goes like $\nu^{1/3}$. We then follow BDM96 and interpret this as optically thin synchrotron radiation of quasi-monoenergetic electrons. The mean electron energy then is fairly well constrained since the maximum of F_ν^{nuc} has to be at frequencies above the K band, but not much higher as otherwise the total nuclear flux from the center of NGC 1068 would be too large. The situation is less clear with the SSA frequency. We cannot rule out that SSA in fact occurs at frequencies even smaller than 5 GHz. As a consequence of this, the source radius discussed below is only a lower limit. For details we refer the reader to BDM96¹.

If we assume that the maximum of F_ν^{nuc} is indeed achieved around $2\ \mu\text{m}$, and that SSA of the source becomes important for frequencies below 5 GHz, we find as emitting region a homogeneous sphere of radius $R \sim 2 \cdot 10^{15}\ \text{cm}$ ($\sim 0.7\ \text{mpc} \sim 130\ \text{AU} \sim 0.01\ \text{mas}$) with a magnetic field $B \sim 11\ \text{G}$ (assumed to be the same everywhere in this region). The relativistic electrons have a number density $n_e \sim 1.1 \cdot 10^3\ \text{cm}^{-3}$, a mean energy $E \sim 2.7\ \text{GeV}$ and a width of the energy distribution $\Delta E/E \sim 1$. In Fig. 5 we show a comparison of the observed fluxes of NGC 1068 core and our model spectrum using the above parameters. If our speculation applies, it turns out that the main difference between NGC 1068 and other galactic centers analysed on the basis of the same interpretation (Sgr A*: BDM96; M 81: Reuter and Lesch 1996; M 104: Jauch and Duschl, in prep.) are the source radius and – especially – the energy of the relativistic electrons. The above size of 0.01 mas means that our resolved 30 mas object is not the synchrotron source itself but rather a larger object, most likely the nuclear torus and/or a circumnuclear scattering halo.

5. Conclusions

We have resolved a compact source with a diameter of $d_{\text{Gauss}} \sim 30\ \text{mas}$ in the core of NGC 1068. This object is most likely a nuclear torus and/or a circumnuclear scattering halo. Part of the radiation from the central 30 mas may be light from the nucleus scattered in the halo. Under this assumption, we were able to determine physical parameters of the nucleus and compare them to other galactic centers, active and non-active ones. One then is tempted to speculate that the higher efficiency of the acceleration mechanism for the electrons may be the true difference between an active galactic center and a normal one.

¹ For other models of such a spectral distribution, we refer to the discussion in MDZ96

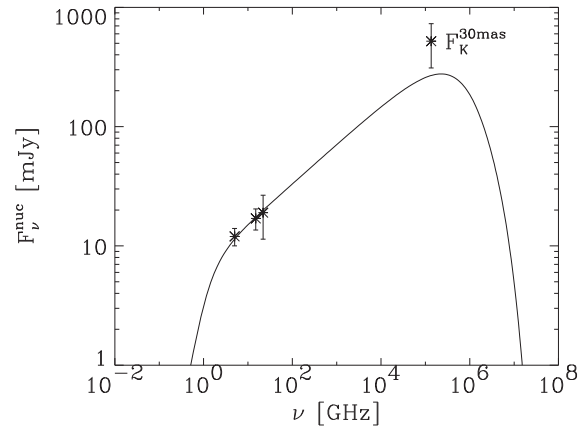


Fig. 5. A comparison of the model spectrum (for parameters, see the text) with flux determinations with a sufficiently high spatial resolution. The fluxes were taken from MPH96 (5 and 22 GHz), Ulvestad, Neff, Wilson (1987; 15 GHz), and the present paper (K-band).

Acknowledgements. We thank Ms. Siân Adey for valuable comments on the manuscript and the referee for many helpful comments concerning the flux determination and other comments. This work was in part supported by the *Deutsche Forschungsgemeinschaft* through Sonderforschungsbereich 328 (*Evolution of galaxies*) at the University of Heidelberg.

References

- Antonucci R.R.J., Miller J.S., 1985, ApJ 297, 621
- Bailey J., et al., 1988, MNRAS 234, 899
- Beckert T., Duschl W.J., Mezger P.G., Zylka R., 1996, A&A 307, 450 (=BDM96)
- Blietz M. et al., 1994, ApJ 421, 92
- Chelli A., Perrier C., Cruz-Gonzalez I., Carrasco L., 1987, A&A 177, 51
- Duschl W.J., Lesch H., 1994, A&A 286, 431
- Elias J.H., Frogel J.A., Matthews K., Neugebauer G., 1982, AJ 87, 7
- Lohmann A.W., Weigelt G., Wirmitzer B., 1983, Appl. Opt. 22, 4028
- Mezger P.G., Duschl W.J., Zylka R., 1996, AAR 7, 289 (=MDZ96)
- Muxlow T.W.B. et al. 1996, MNRAS 278, 854 (=MPH96)
- Pehlemann E., Hofmann K.-H., Weigelt G., 1992, A&A 256, 701
- Quirrenbach A., Eckart A., Thatte N., 1997, "High-resolution near-infrared observations of NGC 1068", preprint
- Tacconi L.J. et al., 1994, ApJ 426, L77
- Thatte N., Quirrenbach A., Genzel R., Maiolino R., Tecza M., 1997, to appear in ApJ
- Ulvestad J.S., Neff S.G., Wilson A.S., 1987, AJ 93, 22
- Weigelt G.P. 1977, Opt Commun. 21, 55
- Weinberger A.J., Neugebauer G., Matthews K., 1996, BAAS 196, 10.05
- Young S., Packham C., Hough J.H., Efsthathiou A., 1996, MNRAS 283, L1